THE JOURNAL OF PHYSICAL CHEMISTRY A

Article

pubs.acs.org/JPCA

Mechanism of the Deamination Reaction of Isoguanine: A Theoretical Investigation

Youqing Yu, Kunhui Liu, Hongmei Zhao, and Di Song*

Beijing National Laboratory for Molecular Sciences (BNLMS), State Key Laboratory of Molecular Reaction Dynamics, Institute of Chemistry, Chinese Academy of Sciences, Beijing 100190, China

Supporting Information

ABSTRACT: Mechanisms of the deamination reactions of isoguanine with H_2O, OH^-, and OH^-/H_2O and of protonated isoguanine ($isoGH^+$) with H_2O have been investigated by theoretical calculations. Eight pathways, paths A–H, have been explored and the thermodynamic properties (ΔE, ΔH, and ΔG), activation energies, enthalpies, and Gibbs energies of activation were calculated for each reaction investigated. Compared with the deamination reaction of isoguanine or protonated isoguanine ($isoGH^+$) with water, the deamination reaction of isoguanine with OH^- shows a lower Gibbs energy of activation at the rate-determining step, indicating that the deamination reaction of isoguanine is favorably to take place for the deprotonated form $isoG^-$ with water. With the assistance of an extra water, the reaction of isoguanine with OH^-/H_2O, pathways F and H, are found to be the most feasible pathways in aqueous solution due to their lowest Gibbs energy of activation of 174.7 and 172.6 kJ mol^{-1}, respectively, at the B3LYP/6-311++G(d,p) level of theory.

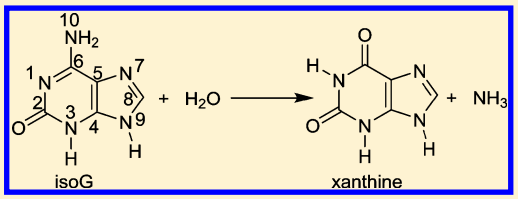

1. INTRODUCTION

One of the most interesting tautomers of purine nucleobases is isoguanine (2-oxo-6-amino-guanine, isoG; Scheme 1), a mutagenic molecule which can be spontaneously formed by oxidative stress of adenine.[1] It has been found to occur naturally.[2,3] The yields of isoG in monomeric form are similar to those of 8-oxoguanine, which is the most frequent lesion observed in DNA or nucleotides.[4,5] Moreover, isoG possesses a similar mutation ability to that of 8-oxoguanine in vivo. Thus, isoG can be considered as another important cause of DNA damage produced by reactive oxygen species (ROS). Isoguanine is mutagenic to *Escherichia coli*.[6,7] This base is incorporated into DNA by DNA polymerase III opposite guanine. The insertion of isoG into DNA increases the rate of mutagenesis,[8−10] which has been related to a similar ability of isoG to recognize cytosine and thymine, leading to pyrimidine transitions. The ability of isoG to recognize guanine and even adenine[1] also explains the C to G and C to A transversions. Mutagenic lesions in cellular DNA accumulate when isoG is not removed from DNA. This causes mutations by misincorporation of nucleotides and may induce mutations at various stages of carcinogenesis.[1,6]

Scheme 1. Deamination Reaction of isoG

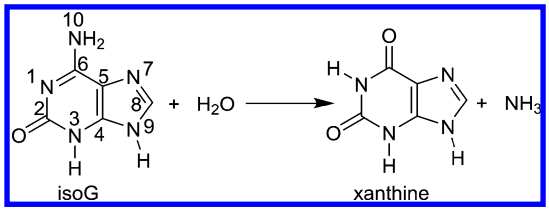

Similar to other nucleic bases, isoG is subject to deamination reaction. Scheme 1 shows the hydrolysis demination of isoG to xanthine. The product xanthine selectively forms base pairs with thymine instead of cytosine, resulting in replicative transition mutation. Meanwhile, ammonia released by the deamination reaction is also toxic to the organism. This strongly indicates deamination of isoG is of biological importance.

In bacteria, deamination of isoG occurs via the cytosine deaminase, generating information on how this deamination reaction takes place in living systems.[11] Among theoretical methods, the multilayered ONIOM computational model provides a further understanding of the mechanism of the deamination reaction by taking into account the catalysis of deaminase. With the ONIOM model, Yao et al. proposed that two-proton shuttles and a Zn metalloenzyme play key roles in the hydrolytic deamination of guanine to xanthine, as catalyzed by guanine deaminase.[12] Sponer et al. investigated the metal-mediated deamination of cytosine with Pt complexes through experimentation and density functional theory (DFT) calculations and reported a much higher activation energy of the rate-determining step, 213.2 kJ mol^{-1}, for cytosine.[13] By including thermal motion into ONIOM-MD calculations, Matsubara et al.[14] showed that the neighboring amino acid residue affects not only the geometry and energy of the substrate but also the elementary step of the catalytic cycle. This is an important factor of the environmental effects to facilitate the deamination reaction.

Received: March 31, 2013
Revised: June 14, 2013
Published: June 21, 2013

dx.doi.org/10.1021/jp4031738 | J. Phys. Chem. A 2013, 117, 5715–5725

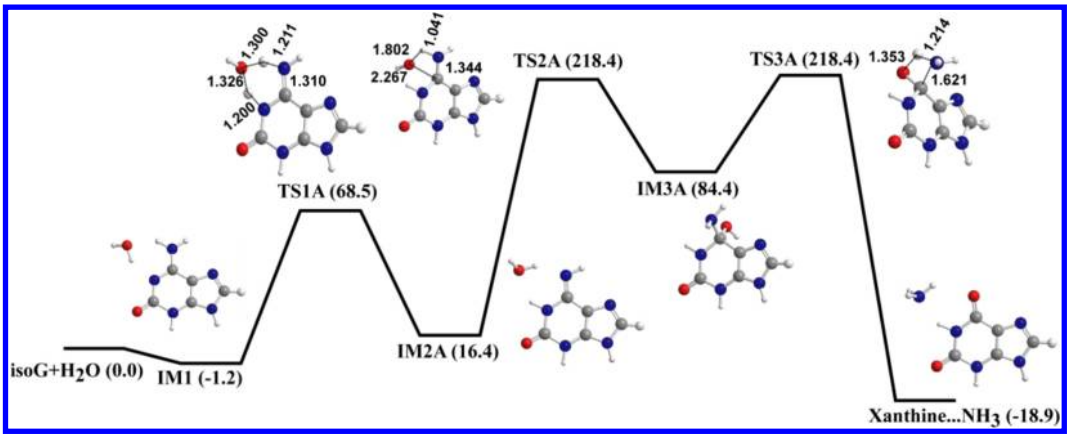

Figure 1. Relative Gibbs energies for the deamination of isoG with H_2O (path A) calculated at the B3LYP/6-311++G(d,p) level (kJ mol^{-1}).

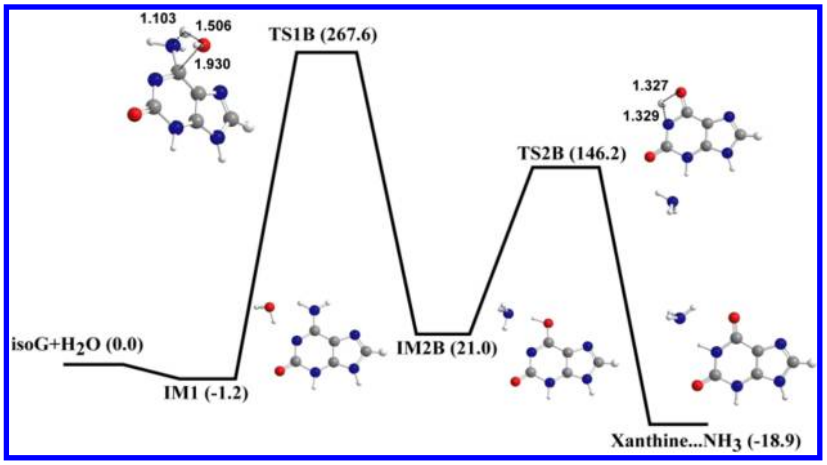

Figure 2. Relative Gibbs energies for the deamination of isoG with H_2O (path B) calculated at the B3LYP/6-311++G(d,p) level (kJ mol^{-1}).

In spite of the crucial role of the deaminase in the deamination reactions of nucleotides, it is still important to have an understanding of how the reaction occurs without catalysis to reveal the catalyzed or uncatalyzed mechanism. Poirier and his co-workers investigated the uncatalyzed deamination reaction of cytosine,[15,16] guanine,[17] 8-oxoguanine,[18] and adenine[19] by quantum chemical calculations. They concluded that the barriers of the uncatalyzed deamination reaction of the nucleic bases decreased with the association of OH^- and would be lowered by participation of extra water. These results provide theoretical evidence for better understanding the catalyzed mechanism.

Experimentally, the kinetic rate constants determined by Hitchcock et al.[11] for the deamination of isoG and cytosine by the cytosine deaminase (k_{cat}/K_m) are $(6.7 \pm 0.3) \times 10^5$ and $(1.5 \pm 0.1) \times 10^5$ M^{-1} s^{-1}, respectively. The value of k_{cat}/K_m for the deamination of isoG is about 4-fold greater than that of cytosine. Hitchcock et al. thus suggested that isoG is the better substrate for the cytosine deaminase under pH = 7.7. However, two factors, the nature of substrate and catalytic selectivity of the cytosine deaminase, have influence on demination of isoG and cytosine in vivo. It remains to be seen which factor play a more important role in the reaction.

To the best of our knowledge, no high level theoretical studies have been reported for the deamination of isoG so far. To gain a clearer understanding of the biological role of isoG, a detailed computational study of the deamination of isoG with H_2O, OH^-, and OH^-/H_2O, and protonated isoG ($isoGH^+$) with H_2O, is presented. Different levels of quantum chemical calculations were performed to ensure the reliability of the current results. The activation energy barriers for the deamination reaction, the hydrolysis of isoG to xanthine, have been obtained by taking into account the form of the substrate (neutral, protonated, or deprotonated form of isoG), the participation of additional water molecules, and the effect of the bulk solvent.

2. COMPUTATIONAL METHODS

The geometries of all reactants, transition states, intermediates, and products were fully optimized at the B3LYP/6-311++G(d,p) level of theory. All the optimizations were once carried out at the HF/6-31+G(d), MP2/6-31+G(d), and B3LYP/6-31+G(d) level of theory. The energies calculated by B3LYP/6-31+G(d) are in good agreement with the MP2 results. Thus, the B3LYP method can be believed to be a balanced method considering the computational efficiency and accuracy. For more accurate energetic information, this work chooses the B3LYP method with a larger basis set (6-311++G(d,p)) to optimize geometries and calculate energies. To ensure the accuracy of energies obtained, the energetic information for the deamination of isoG with OH^-/H_2O (paths F and H) are further refined using the G3MP2 method. The B3LYP/6-311++G(d,p) results agree well with the G3MP2 results, indicating B3LYP/6-311++G(d,p) can provide similar results with lower computation consume. All the detailed geometry parameters and energies are given in the Supporting Information.

The harmonic frequency analysis was used to confirm the stationary point as the minimum with all positive frequencies, or

dx.doi.org/10.1021/jp4031738 | J. Phys. Chem. A 2013, 117, 5715−5725

Table 1. Activation Energies, Enthalpies of Activation, and Gibbs Energies of Activation for the Deamination of Isoguanine with H_2O (kJ mol^{-1}) at 298.15 K (Paths A and B)[a]

		B3LYP/6-311++G(d,p)	PCM/B3LYP/6-311++G(d,p)
path A	$\Delta E_{a,TS1A}$	61.4	58.5
	$\Delta H^{\#}_{TS1A}$	57.3	56.8
	$\Delta G^{\#}_{TS1A}$	69.7	62.3
	$\Delta E_{a,TS2A}$	196.9	171.0
	$\Delta H^{\#}_{TS2A}$	194.8	169.3
	$\Delta G^{\#}_{TS2A}$	202.0	183.9
	$\Delta E_{a,TS3A}$	138.8	123.3
	$\Delta H^{\#}_{TS3A}$	137.1	122.0
	$\Delta G^{\#}_{TS3A}$	134.0	125.0
	$\Delta G^{\#}_{overall}$	219.6	192.6
path B	$\Delta E_{a,TS1B}$	259.2	206.9
	$\Delta H^{\#}_{TS1B}$	255.4	233.7
	$\Delta G^{\#}_{TS1B}$	268.8	240.8
	$\Delta E_{a,TS2B}$	124.6	137.1
	$\Delta H^{\#}_{TS2B}$	125.0	137.5
	$\Delta G^{\#}_{TS2B}$	125.2	136.3
	$\Delta G^{\#}_{overall}$	268.8	240.0

[a]Barriers were calculated from the isoG···H_2O (IM1) complex as defined in Figures 1 and 2.

Scheme 2. Reaction Mechanism for the Deamination of isoG with H_2O (Paths A and B)

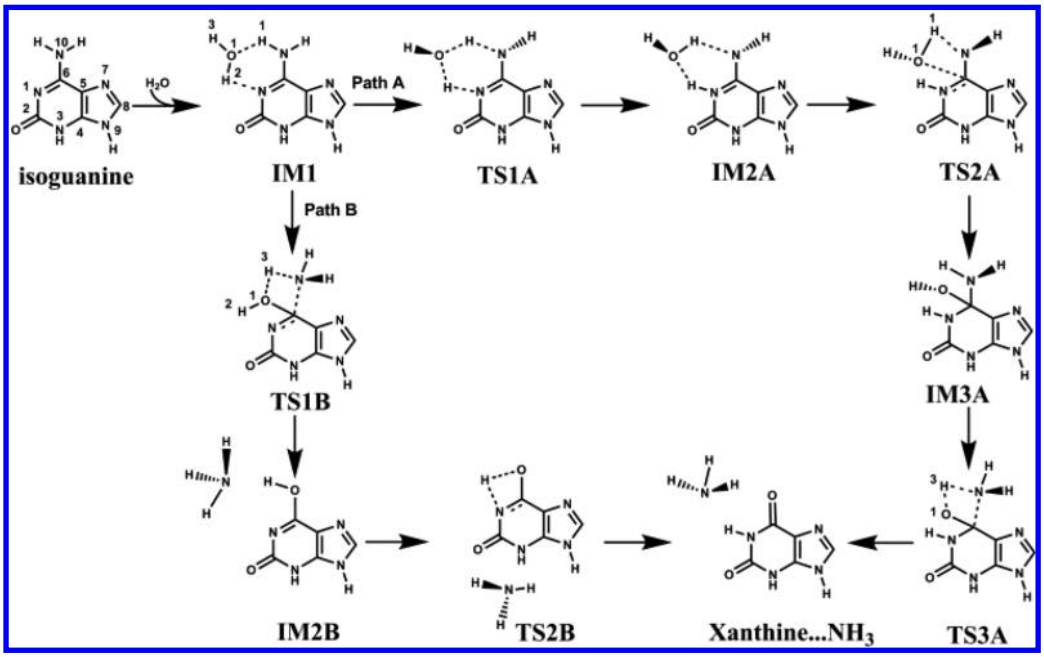

as a transition state with only one imaginary frequency. Connections of the transition states between two local minima have been confirmed by intrinsic reaction coordinate (IRC) calculations.[20] Bulk solvation effects were simulated by using the polarized continuum model PCM at B3LYP/6-311++G(d,p) level.[21] All calculations were performed by using the Gaussian 03 program.[22]

3. RESULTS AND DISCUSSION

The results for the deamination reaction of isoG with H_2O, OH^-, and OH^-/H_2O and $isoGH^+$ with H_2O at B3LYP/6-311++G(d,p) level are given in Tables 1−4. Along the potential energy surfaces of the deamination reaction of isoG, the geometries optimized, and relative energies for all stationary points and saddle points are presented in Figures 1−8.

3.1. Deamination Reaction of isoG with H_2O: Reaction of the Neutral Form (isoG). Figures 1 and 2 show the optimized structures of the reactant, intermediates, transition states, and products for the deamination reaction of isoG with H_2O. The relative activation energies, Gibbs energies, and enthalpies are collected in Table 1. Starting from the complex of isoG with H_2O, namely, IM1, two pathways are obtained, labeled as paths A and B (as shown in Scheme 2, Figure 1, and Figure 2), respectively. In path A, TS1A, which results in a proton transfer from the NH_2 moiety to the N1 atom, has a Gibbs energy of activation of 69.7 kJ mol^{-1}. Following the proton transfer, a nucleophilic addition of the hydroxyl group to the C6 carbon occurs simultaneously with a proton transfer from H_2O to the imine nitrogen via the four-membered ring transition state, TS2A, leading to the formation of IM3A. This step is rate-determining step with a Gibbs energy of activation of 202.0 kJ

dx.doi.org/10.1021/jp4031738 | J. Phys. Chem. A 2013, 117, 5715−5725

mol^{-1}. Finally, the product complex of xanthine and ammonia is yielded via another proton transfer transition state, TS3A, with a Gibbs energy of activation of 134.0 kJ mol^{-1}. The overall Gibbs energy of activation for path A is 219.6 kJ mol^{-1}.

In path B, also starting from the complex of isoG and H_2O, IM1, the C6 atom of isoG undergoes direct nucleophilic attack by water and a simultaneous rupture of the C6−N10 single bond to form the intermediate, IM2B, via TS1B. This step is a rate-determining step with a Gibbs energy of activation of 268.8 kJ mol^{-1}. Finally, the hydrogen atom of the hydroxyl group transfers to the N1 atom to form the xanthine···NH_3 complex through TS2B with a Gibbs energy of activation of 125.2 kJ mol^{-1}.

3.2. Deamination Reaction of Protonated isoG (isoGH$^+$) with H_2O: Reaction of the Protonated Form (isoGH$^+$). For the protonated isoG, three structures, isoGH$^+$ (N1), isoGH$^+$ (N7), and isoGH$^+$ (N10), can be obtained when protons are added to different sites of isoG, as shown in Scheme 3. The

Scheme 3. Protonated and Deprotonated Sites of isoG

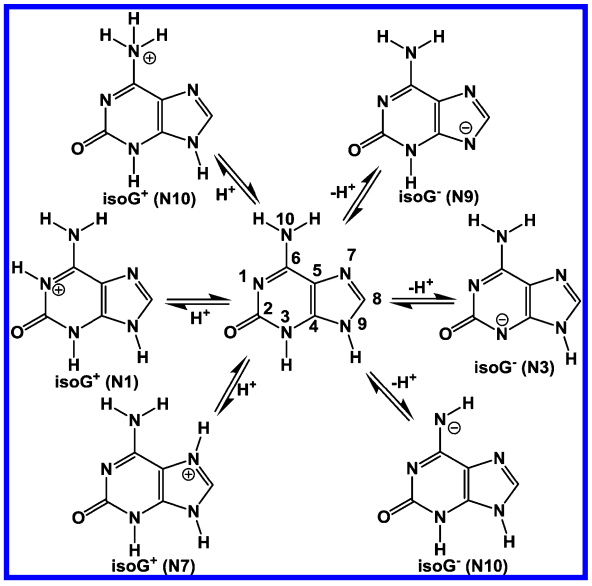

proton affinities (PAs) of N1, N7, and N10 can be defined as the change of enthalpy. The computed PA values of N1, N7, and N10 of isoG are 974.4, 887.0, and 836.8 kJ mol^{-1}, respectively, at the B3LYP/6-311++G(d,p) level of theory.

From the two protonated isoG tautomers, isoGH$^+$ (N10) and isoGH$^+$ (N1), which can undergo the deamination reaction, two possible pathways are obtained, labeled as paths C and D (as shown in Scheme 4), respectively. The relative energies and optimized structures of the reactant, intermediates, transition states, and product for paths C and D are shown in Figures 3 and 4. The activation energies, Gibbs energies, and enthalpies of paths C and D are listed in Table 2.

For path C, the water molecule forms a reactant complex with isoGH$^+$(N10), IM2C, through electrostatic interaction. Initially, the water molecule attacks the C6 atom by simultaneously dissociating the ammonium group NH_4^+ from isoG, yielding the hydroxyl tautomer of xanthine and the ammonium group. This step occurs via the transition state, TS1C, which corresponds to a high Gibbs energy of activation of 220.5 kJ mol^{-1} and can be considered as the rate-determining step for the whole path C. After that, the hydroxyl tautomer of xanthine eventually transforms into the final product of xanthine, via the intramolecular proton transfer transition state, TS2C, with a low Gibbs energy of activation of 112.6 kJ mol^{-1}.

In path D, starting from the reactant complex, IM2D, which is formed between water and the N1-protonated isoG, isoGH$^+$ (N1), nucleophilic addition of H_2O to C6 with a simultaneous proton transfer from H_2O to the nitrogen atom of the amine group (TS1D) forms a tetrahedral intermediate, IM3D. To dissociate the ammonia group from the C6 atom, a very low barrier (almost 0.0 kJ mol^{-1}) transition state, TS2D, which connects IM3D and IM4D, is identified. The whole path D is rate-limited by TS1D, with a Gibbs energy of activation of 269.7 kJ mol^{-1}.

Additionally, the initial complex of IM2C in path C can transform to the path D complex of IM2D through an intramolecular proton transfer from the N10 atom to the N1 atom, with a six-membered ring transition state TS1. The Gibbs energy of activation for this step is only 28.8 kJ mol^{-1}, indicating that paths C and D can be easily linked together.

3.3. Deamination Reaction of isoG with OH$^-$ or OH$^-$/H_2O: Reaction of the Deprotonated Form (isoG$^-$). In the presence of OH$^-$, isoG undergoes deprotonation, generating the complex of isoG anion (isoG$^-$) and H_2O. Scheme 3 shows that the three deprotonation sites, N3, N9 or N10 of isoG. The corresponding deprotonation enthalpies [PA(A$^-$)] are 1409.1, 1344.8, and 1472.5 kJ mol^{-1} at the B3LYP/6-311++G(d,p) level, respectively. Deprotonation of isoG at the N3 and N10 site were considered, as the N9 site of isoguanie is connected to a sugar ring. In this case, two paths were found for deamination reaction of isoG with OH$^-$, labeled as E and G. Path E corresponds to the deamination reaction that starts from the isoG$^-$(N3)/H_2O complex (IM2E), whereas path G shows the deamination reactions starting from the isoG$^-$(N10)/H_2O (IM2G). Because previous works suggested that the energy barriers for deamination reactions involving proton transfer are usually lowered in the presence of additional water,[15,16] another two paths, designed as F and H, were studied for the deamination reaction of isoG with H_2O/OH$^-$. Paths F and H represent the deamination reaction of paths E and G assisted by an additional water molecule, respectively. The relative energies and optimized structures of the reactants, intermediates, transition states, and products for paths E−H are shown in Figures 5−8, respectively. The activation energies, Gibbs energies, and enthalpies of paths E−H are listed in Tables 3 and 4.

In path E, as shown in Figure 5 and Scheme 5, IM2E first undergoes proton transfer from the NH_2 moiety to the N1 atom, via a six-membered ring transition state, TS1E, with a low Gibbs energy of activation of 37.4 kJ mol^{-1}. Subsequently, the C6 carbon atom of IM3E undergoes nucleophilic attack by the oxygen atom of H_2O, which is accompanied by a simultaneous proton transfer from H_2O to the N10 atom of IM3E via a four-membered ring transition state, TS2E. This step faces a Gibbs energy of activation of 181.0 kJ mol^{-1}, leading to the formation of IM4E. To dissociate the amine group of IM4E, the hydrogen atom of the hydroxyl group must transfer to the N10 atom and rupture the C6−N10 bond through the four-membered ring transition state, TS3E, with a Gibbs energy of activation of 97.0 kJ mol^{-1}. An overall Gibbs energy of activation of 198.6 kJ mol^{-1} is required for path E (from IM2E to TS3E).

In Path F (Figure 6 and Scheme 6), the isoG$^-$(N3)/2H_2O complex, IM2F, undergoes proton transfer from the N10 atom to the N1 atom through the eight-membered ring transition state, TS1F. The Gibbs energy of activation for this step is 31.5 kJ mol^{-1}, very close to that of TS1E observed in path E. Following

dx.doi.org/10.1021/jp4031738 | J. Phys. Chem. A 2013, 117, 5715−5725

Scheme 4. Reaction Mechanism for the Deamination of Protonated isoG (isoGH$^+$) (Paths C and D) with H_2O

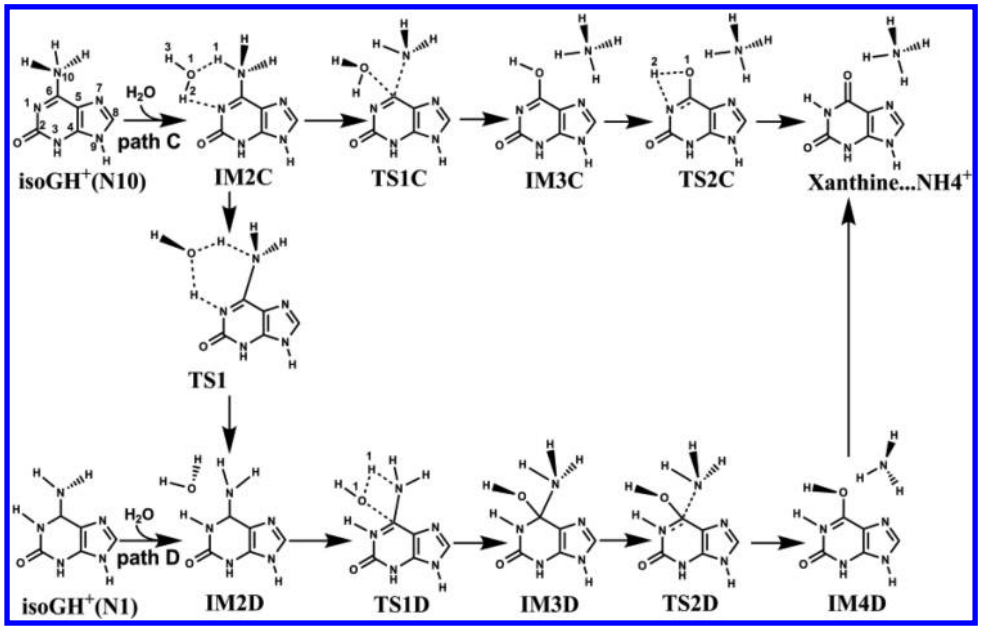

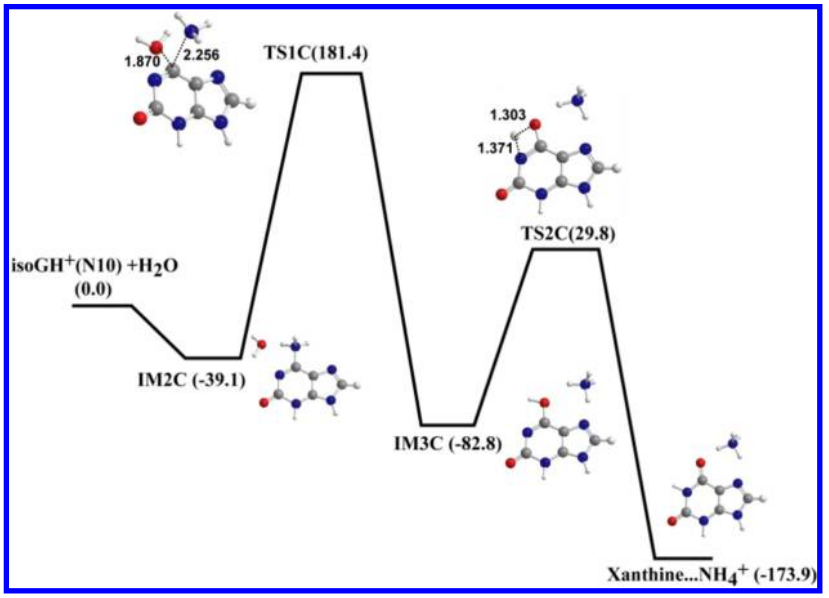

Figure 3. Relative Gibbs energies for the deamination of protonated isoG (isoGH$^+$) with H_2O (path C) calculated at the B3LYP/6-311++G(d,p) level (kJ mol^{-1}).

the proton transfer, the nucleophilic attack of water to C6 carbon atom occurs through a six-membered ring transition state, TS2F, with the assistance of the additional water. The Gibbs energy of activation for this step is 147.4 kJ mol^{-1}, which is lower than that of TS2E observed in path E by about 33.6 kJ mol^{-1}. This is attributed to the six-membered ring structure of TS2F, which has a reduced likelihood of the structural deformation than the four-membered ring structure of TS2E involved in path E, thereby resulting in a lowering of the Gibbs energy of activation of path F.

After the nucleophilic addition of H_2O, the bond rupture of C6−N10 occurs via the six-membered ring transition state, TS3F, with the activation free energy of 73.1 kJ mol^{-1}, which is about 23.9 kJ mol^{-1} lower than that of TS3E in path E. This indicates that the second water also assists the bond rupture step. Overall, the energy barriers in path F are lower than those in path E, due to the participation of the additional water. It requires an overall Gibbs energy of activation of 185.2 kJ mol^{-1} (from IM2F to TS3F) to surmount in path F.

Similarly, paths G and H correspond to the deamination reactions starting from the isoG$^-$(N10)/H_2O (IM2G) and isoG$^-$(N10)/2H_2O (IM2H) complexes, respectively (Figure 7, Figure 8, and Scheme 7). In path G, IM2G undergoes nucleophilic attack of the C6═N10 double bond by water, resulting in the formation of the tetrahedral intermediate, IM3G, via the transition state, TS1G, with a Gibbs energy of activation of 159.2 kJ mol^{-1}. Subsequently, the C6−N10 bond is ruptured as a result of the proton transfer from OH to the N10 atom through transition state TS2G, with a Gibbs energy of activation of 104.2 kJ mol^{-1}. An overall Gibbs energy of activation of 210.8 kJ mol^{-1} (from IM2G to TS2G) is required to overcome for this pathway.

dx.doi.org/10.1021/jp4031738 | J. Phys. Chem. A 2013, 117, 5715−5725

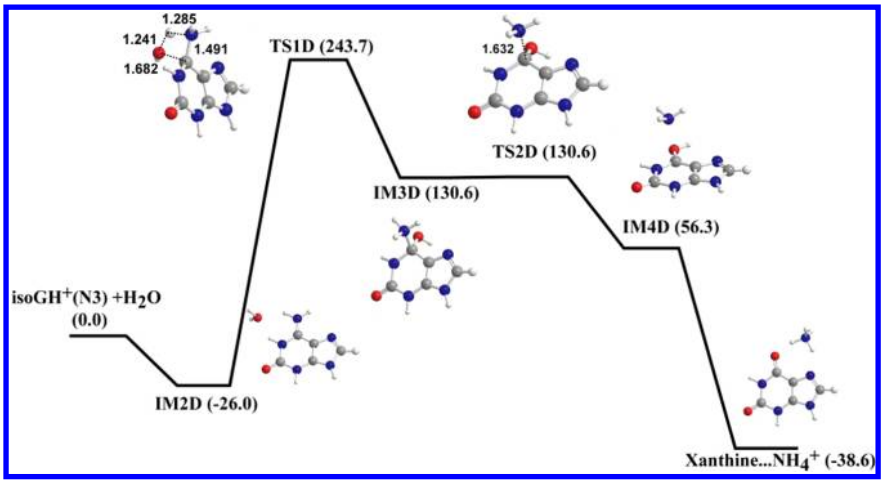

Figure 4. Relative Gibbs energies for the deamination of protonated isoG (isoGH$^+$) with H_2O (path D) calculated at the B3LYP/6-311++G(d,p) level (kJ mol^{-1}).

Table 2. Activation Energies, Enthalpies of Activation, and Gibbs Energies of Activation for the Deamination of Protonated Isoguanine (isoGH$^+$) with H_2O (kJ mol^{-1}) at 298.15 K (Paths C[a] and D[b])

		B3LYP/6-311++G(d,p)	PCM/B3LYP/6-311++G(d,p)
path C	$\Delta E_{a,TS1}$	20.5	25.1
	$\Delta H^{\#}_{TS1}$	15.5	24.2
	$\Delta G^{\#}_{TS1}$	28.8	27.2
	$\Delta E_{a,TS1C}$	216.9	222.8
	$\Delta H^{\#}_{TS1C}$	218.2	227.4
	$\Delta G^{\#}_{TS1C}$	220.5	217.4
	$\Delta E_{a,TS2C}$	110.4	126.2
	$\Delta H^{\#}_{TS2C}$	109.5	127.1
	$\Delta G^{\#}_{TS2C}$	112.6	123.7
	$\Delta G^{\#}_{overall}$	220.5	217.4
path D	$\Delta E_{a,TS1D}$	264.2	247.0
	$\Delta H^{\#}_{TS1D}$	260.0	242.4
	$\Delta G^{\#}_{TS1D}$	269.7	253.3
	$\Delta E_{a,TS2D}$	−1.7	0.4
	$\Delta H^{\#}_{TS2D}$	−2.9	−0.8
	$\Delta G^{\#}_{TS2D}$	0	1.7
	$\Delta G^{\#}_{overall}$	269.7	253.3

[a]Barriers were calculated from the isoGH$^+$(N10)···H_2O (IM2C) complex as defined in Figure 3. [b]Barriers were calculated from the isoGH$^+$(N1)···H_2O (IM2D) complex as defined in Figure 4.

Path H is also a two-step mechanism. The first step of nucleophilic addition of water to the C6═N10 double bond occurs through a six-membered ring structure, TS1H, with a Gibbs energy of activation of 128.9 kJ mol^{-1}. Compared to the Gibbs energy of activation of TS1G in path G, the barrier of TS1H is decreased by 30.3 kJ mol^{-1} as a result of the assistance provided by the additional water molecule. The second step of dissociation is also facilitated by the additional water, with a Gibbs energy of activation of 93.2 kJ mol^{-1}, which is decreased by 11.0 kJ mol^{-1} relative to TS2G.

3.4. Comparison of Deamination Reactions for Different Forms of isoG. Our calculations have revealed six reaction pathways for the deamination of different forms of isoG with H_2O, labeled as paths A and B (neutral), paths C and D (protonated), and paths E and G (deprotonated), with the overall Gibbs energies of activation of 219.6 (TS2A), 268.8 (TS1B), 220.5 (TS1C), 269.7 (TS1D), 198.6 (TS3E), and 210.8 (TS2G) kJ mol^{-1}, respectively. These results suggest that the deamination reaction is more likely to occur for the deprotonated form of isoG than for the neutral or protonated forms. This may be attributed to the increasing electronegativity of isoG$^-$ after the deprotonation by OH$^-$, which results in a significantly lowered barrier of transition states.

Furthermore, the deamination reaction of isoG with OH$^-$ can be enhanced by the participation of additional water, as shown with the calculated paths F and H. This is ascribed to the reason that the water molecule can stabilize the transition states, which is agreement with previous results.[23] Due to the assistance provided by the additional water, the overall Gibbs energies of activation for pathways F and H are lowered to 185.2 (TS3F) and 193.2 (TS2H) kJ mol^{-1}, respectively. Such small energy differences of 8.0 kJ mol^{-1} may result from the theoretical calculation error. Thus, paths F and H, the deamination of isoG with OH$^-$/H_2O, can be considered as the two most feasible pathways. This is in line with the results of mechanistic investigations on the deamination of cytosine, guanine, and 8-oxoguanine.[17,18] For these four molecules, OH$^-$ seems to be essential for the deamination. However, a recent study reported that the most plausible mechanism is the deamination of adenine with 3H_2O, rather than adenine with OH$^-$/3H_2O.[19] To further

dx.doi.org/10.1021/jp4031738 | J. Phys. Chem. A 2013, 117, 5715−5725

Table 3. Activation Energies, Enthalpies of Activation, and Gibbs Energies of Activation for the deamination of isoguanine (isoG) with OH^- or OH^-/H_2O (kJ mol^{-1}) at 298.15 K (Paths E[a] and F[b])

		B3LYP/6-311++G(d,p)	G3MP2	PCM/B3LYP/6-311++G(d,p)
path E	$\Delta E_{a,TS1E}$	31.3		28.0
	$\Delta H^{\#}_{TS1E}$	28.4		27.6
	$\Delta G^{\#}_{TS1E}$	37.4		28.8
	$\Delta E_{a,TS2E}$	170.1		145.9
	$\Delta H^{\#}_{TS2E}$	167.2		145.0
	$\Delta G^{\#}_{TS2E}$	181.0		152.6
	$\Delta E_{a,TS3E}$	97.0		110.8
	$\Delta H^{\#}_{TS3E}$	97.4		109.9
	$\Delta G^{\#}_{TS3E}$	97.0		109.1
	$\Delta G^{\#}_{overall}$	198.6		211.1
path F	$\Delta E_{a,TS1F}$	24.2	41.4	20.1
	$\Delta H^{\#}_{TS1F}$	20.1	37.2	16.3
	$\Delta G^{\#}_{TS1F}$	31.5	48.5	26.8
	$\Delta E_{a,TS2F}$	140.0	142.5	125.0
	$\Delta H^{\#}_{TS2F}$	137.1	139.2	120.0
	$\Delta G^{\#}_{TS2F}$	147.4	152.6	135.8
	$\Delta E_{a,TS3F}$	66.9	89.4	60.2
	$\Delta H^{\#}_{TS3F}$	63.5	86.1	58.1
	$\Delta G^{\#}_{TS3F}$	73.1	95.7	64.4
	$\Delta G^{\#}_{overall}$	185.2	182.2	174.7

[a]Barriers were calculated from the $isoG^-(N3)\cdots H_2O$ (IM2E) complex as defined in Figure 5. [b]Barriers were calculated from the $isoG^-(N3)\cdots 2H_2O$ (IM2F) complex as defined in Figure 6.

Table 4. Activation Energies, Enthalpies of Activation, and Gibbs Energies of Activation for the Deamination of Isoguanine (isoG) with OH^- or OH^-/H_2O (kJ mol^{-1}) at 298.15 K (Paths G[a] and H[b])

		B3LYP/6-311++G(d,p)	G3MP2	PCM/B3LYP/6-311++G(d,p)
path G	$\Delta E_{a,TS1G}$	151.3		117.4
	$\Delta H^{\#}_{TS1G}$	150.1		117.9
	$\Delta G^{\#}_{TS1G}$	159.2		119.5
	$\Delta E_{a,TS2G}$	104.5		99.9
	$\Delta H^{\#}_{TS2G}$	105.3		99.9
	$\Delta G^{\#}_{TS2G}$	104.2		99.9
	$\Delta G^{\#}_{overall}$	210.8		195.6
path H	$\Delta E_{a,TS1H}$	120.0	120.4	110.8
	$\Delta H^{\#}_{TS1H}$	116.2	116.6	104.1
	$\Delta G^{\#}_{TS1H}$	128.9	129.6	112.4
	$\Delta E_{a,TS2H}$	89.4	110.4	58.5
	$\Delta H^{\#}_{TS2H}$	87.4	107.8	54.8
	$\Delta G^{\#}_{TS2H}$	93.2	112.9	65.2
	$\Delta G^{\#}_{overall}$	193.2	199.0	172.6

[a]Barriers were calculated from the $isoG^-(N10)\cdots H_2O$ (IM2G) complex as defined in Figure 7. [b]Barriers were calculated from the $isoG^-(N10)\cdots 2H_2O$ (IM2H) complex as defined in Figure 8.

determine the role of OH^- in the deamination of isoG, we calculated the deamination mechanisms of isoG with $3H_2O$ and isoG with $OH^-/3H_2O$ (designed as paths I and J), based on paths A and F. The relative energies and optimized structures are shown in Figure S1 and Figure S2 (Supporting Information), and the activation energies, Gibbs energies, and enthalpies are listed in Table S4 and Table S5 (Supporting Information). As shown in Figure S1 and S2 (Supporting Information), the overall Gibbs energies of activation for paths I and J are 178.9 and 168.5 kJ mol^{-1}, implying the deamination reaction of isoguanine is easier to occur in the present of OH^-. These results indicate that OH^- plays more important role in the decreasing energy barriers for deamination of isoG than the addition of H_2O.

The use of continuum models is likely to further lower these barriers. We employed the polarizable continuum model (PCM) to simulate the environmental effect on the energy barriers for the deamination of isoG at B3LYP/6-311++G(d,p) level. Except for path E that slightly increases from 198.6 to 211.1 kJ mol^{-1}, the overall Gibbs energies of activation for paths A−H go down to 192.6, 240.0, 217.4, 253.3, 174.7, 195.6, and 172.6 kJ mol^{-1} and are lower by 27.0, 28.8, 3.1, 16.4, 10.5, 15.2, and 20.6 kJ mol^{-1} compared with the results of the gas phase, respectively. This indicates the water bulk effect can also decrease Gibbs energies of activation for deamination. In other words, the water bulk effect also plays an important role in stabilizing the transition states, as well as the addition of a water molecule. Although the water bulk effect significantly reduces energy barriers for deamination, the most feasible pathways in aqueous are still paths F and H, i.e., the reaction of isoG with OH^-/H_2O, with the lowest energy barriers of 174.7 and 172.6 kJ mol^{-1}.

dx.doi.org/10.1021/jp4031738 | J. Phys. Chem. A 2013, 117, 5715−5725

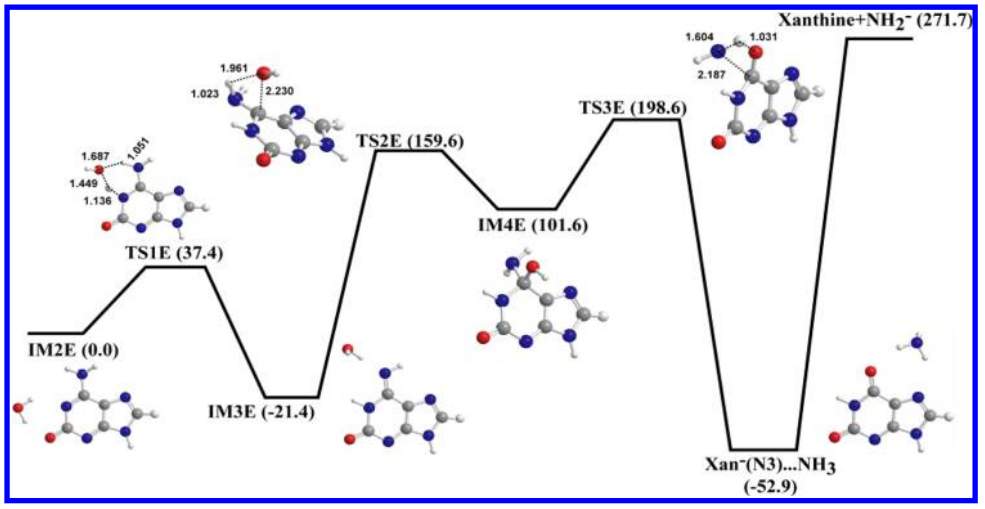

Figure 5. Relative Gibbs energies for the deamination of isoG with OH^- (path E) calculated at the B3LYP/6-311++G(d,p) level (kJ mol^{-1}).

Scheme 5. Reaction Mechanism for the Deamination of isoG with OH^- (Path E)

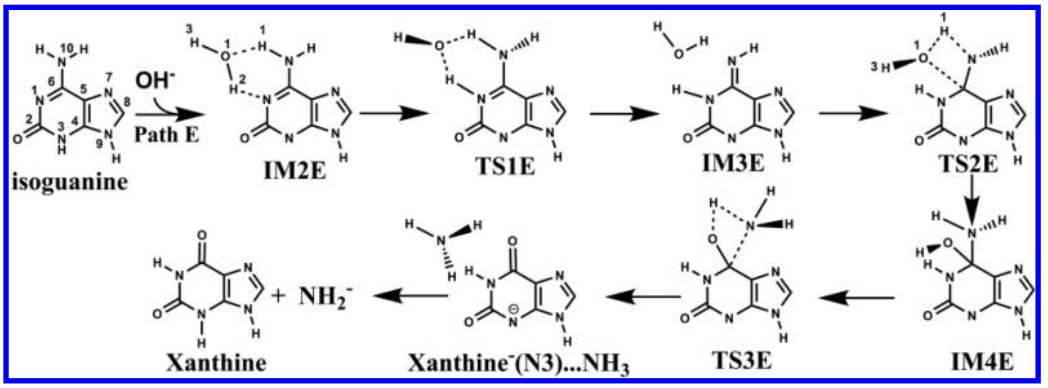

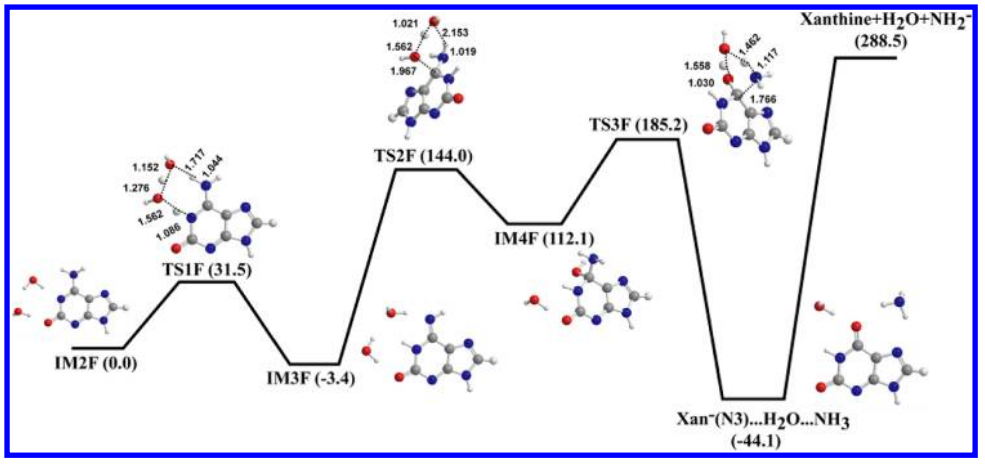

Figure 6. Relative Gibbs energies for the deamination of isoG with OH^-/H_2O (path F) calculated at the B3LYP/6-311++G(d,p) level (kJ mol^{-1}).

For the two most feasible paths F and H, the single point energies are refined using the G3MP2 method, which are summarized in Tables 3 and 4. This allows us to make comparisons with previous theoretical results calculated at the G3MP2 level. As shown in Tables 3 and 4, the overall Gibbs energies of activation for paths F and H are separately 182.2 and 199.0 kJ mol^{-1}. These values are higher than that of the most feasible deamination pathway for cytosine with OH^-/H_2O (122.0 kJ mol^{-1}), implying that isoG seems to be not a better substrate than cytosine in vivo. The catalytic selectivity may be responsible for experimental value of k_{cat}/K_m for the deamination of isoG being 4-fold greater than that of cytosine.[11] From Tables 3 and 4, it can also be found that the activation energies (ΔE_a) for paths F and H are 170.5 and 186.4 kJ mol^{-1}, respectively. The result is close to that of the most likely pathways for deamination of 8-oxoG (187.0 kJ mol^{-1}), but much higher than that of the most likely pathways for deamination of guanine (144.0 kJ mol^{-1}). This seems to show the deamination of guanine is easier to occur.

dx.doi.org/10.1021/jp4031738 | J. Phys. Chem. A 2013, 117, 5715−5725

Scheme 6. Reaction Mechanism for the Deamination of isoG with OH^-/H_2O (Path F)

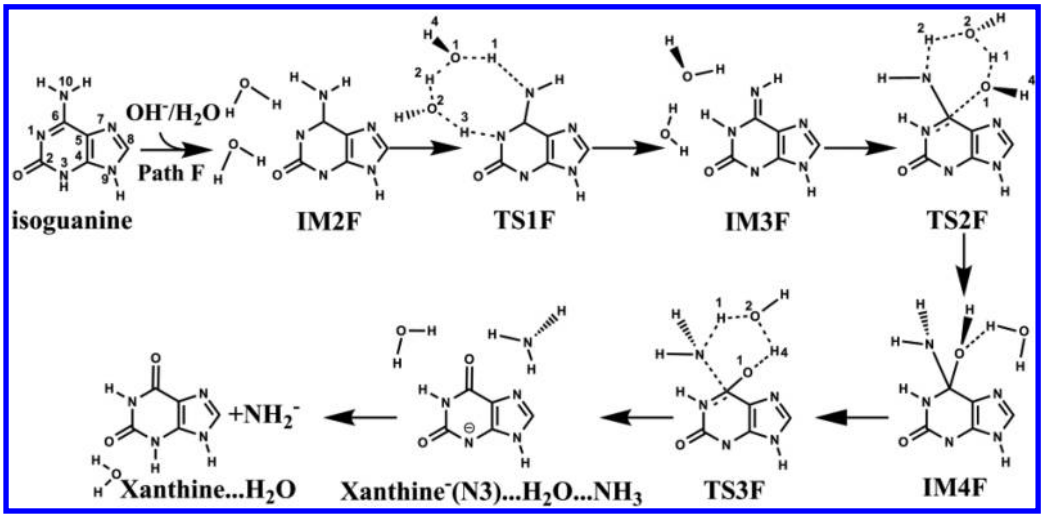

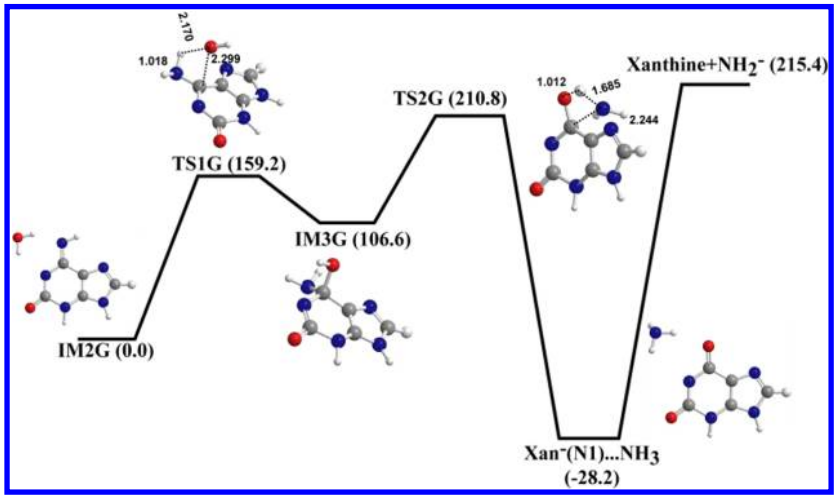

Figure 7. Relative Gibbs energies for the deamination of isoG with OH^- (path G) calculated at the B3LYP/6-311++G(d,p) level (kJ mol^{-1}).

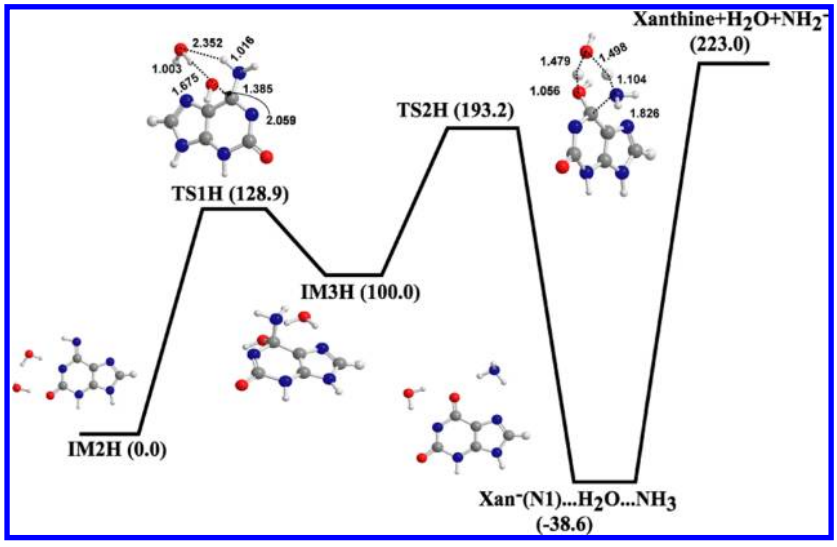

Figure 8. Relative Gibbs energies for the deamination of isoG with OH^-/H_2O (path H) calculated at the B3LYP/6-311++G(d,p) level (kJ mol^{-1}).

3.5. Thermodynamic Properties for the Deamination of isoG. The thermodynamic properties for the deamination reaction of isoG can also be obtained from the B3LYP/6-311++G(d,p) calculations. For the deamination reaction of isoG with H_2O (paths A and B), the Gibbs free energy (ΔG) forming the final product of xanthine$\cdots NH_3$ is −18.9 kJ mol^{-1}. The

dx.doi.org/10.1021/jp4031738 | J. Phys. Chem. A 2013, 117, 5715−5725

Scheme 7. Reaction Mechanism for the Deamination of isoG with OH^- or OH^-/H_2O (Paths G and H)

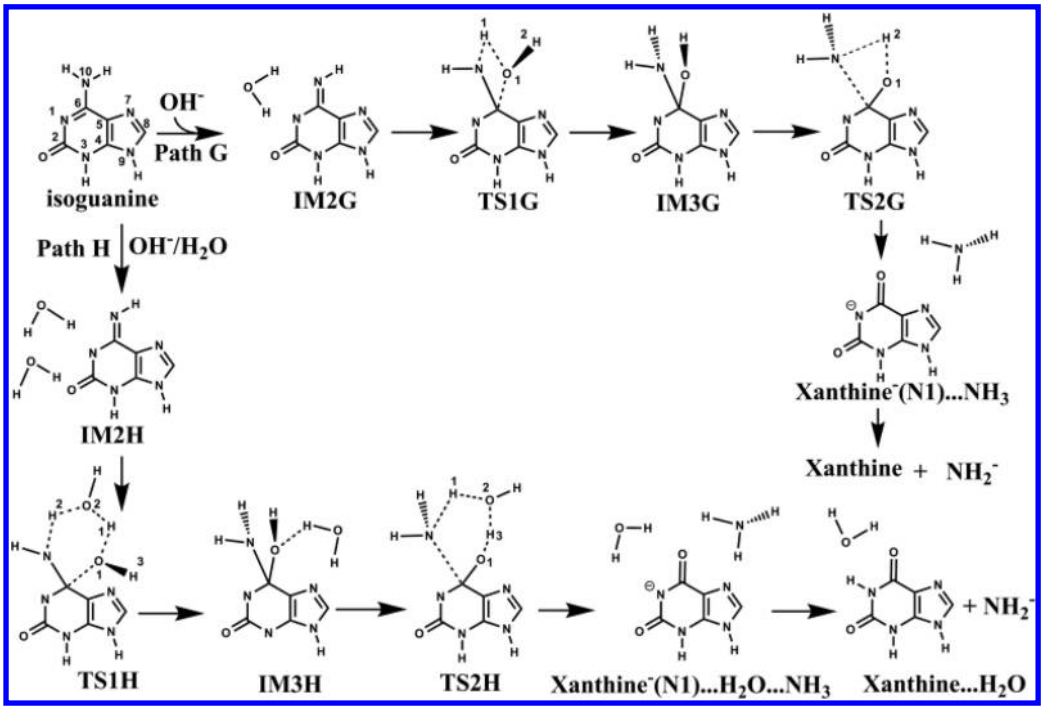

deamination reactions of protonated isoG ($isoGH^+$) with H_2O (paths C and D) have Gibbs free energies (ΔG) of −173.9 and −38.6 kJ mol^{-1}, yielding the complex of xanthine···NH_4^+ as the final product. Deamination of isoG with OH^- to produce the Xan^-···NH_3 complex is found to be exothermic and exergonic, with Gibbs free energies of −294.8 and −213.8 kJ mol^{-1} for paths E and G, respectively. Deamination of isoG with OH^-/H_2O to produce the Xan^- ···NH_3···H_2O complex is also exothermic and exergonic, with Gibbs free energies of −302.8 and −231.8 kJ mol^{-1} for paths F and H, respectively.

4. CONCLUSIONS

The deamination reaction mechanisms of isoguanine (isoG) with H_2O, OH^-, and OH^-/H_2O, and the deamination reaction mechanisms of protonated isoG ($isoGH^+$) with H_2O, were investigated using density functional theory calculations. Optimized geometries were determined at the B3LYP/6-311++G(d,p) levels of theory. Activation energies, enthalpies, and Gibbs energies were calculated for each reaction pathway. For the deamination of isoG with H_2O (pathways A and B), and the deamination of protonated isoG ($isoGH^+$) with H_2O (pathways C and D), the reaction is rate-limited by the nucleophilic addition of water to the C═N double bond, which corresponds to high energy barriers of 219.6 (TS2A), 268.8 (TS1B), 220.5 (TS1C), and 269.7 (TS1D) kJ mol^{-1}, respectively. In contrast, the deamination of isoG with OH^-, the reaction of the deprotonated form ($isoG^-$), has lowered activation energy barriers. The computed overall Gibbs energies of activation for paths E and G are 198.6 (TS3E) and 210.8 (TS2G) kJ mol^{-1}, respectively. After the addition of a water molecule, these values are lowered to 185.2 (TS3F) and 193.2 (TS2H) kJ mol^{-1} for pathways F and H, respectively. It is clear that the participation of one additional water molecule in the reaction is crucial for decreasing the energy barriers and increasing the reaction rate.

Such findings imply that the deamination reaction of isoG is more likely to occur with the deprotonated form of isoG than with the neutral or protonated forms. With the assistance of additional water, the reaction of isoG with OH^-/H_2O, pathways F and H, are found to be the most feasible pathways in the gas phase and in aqueous solution due to their lowest overall Gibbs energies of activation of 174.7 and 172.6 kJ mol^{-1}. In addition, aqueous conditions play a key role in accelerating the deamination reaction rate but do not alter the mechanism. Compared with the case for cytosine, the higher overall activation energies of the most likely pathways of the deamination reaction of isoG implies that deamination of isoG being more likely to occur than cytosine in vivo results from the catalytic selectivity of CDA, rather than the nature of substrates.

■ ASSOCIATED CONTENT

Supporting Information

Full ref 22. Full geometries, reaction mechanisms, and energies of all structures are reported. This material is available free of charge via the Internet at http://pubs.acs.org.

■ AUTHOR INFORMATION

Corresponding Author

*Telephone: +86 01062562837. Fax: +86 01062563167. E-mail: songdi@iccas.ac.cn.

Notes

The authors declare no competing financial interest.

■ ACKNOWLEDGMENTS

This work is financially supported by the National Natural Science Foundation of China (Grant Nos. 20973179, 21003134, 21073201, and 21203206) and the Chinese Academy of Sciences.

■ REFERENCES

(1) Kamiya, H. Mutagenic Potentials of Damaged Nucleic Acids Produced by Reactive Oxygen/Nitrogen Species: Approaches Using

Synthetic Oligonucleotides and Nucleotides. *Nucleic Acids Res.* **2003**, *31*, 517−531.
(2) Chaput, J. C.; Switzer, C. A DNA Pentaplex Incorporating Nucleobase Quintets. *Proc. Natl. Acad. Sci. U. S. A.* **1999**, *96*, 10614−10619.
(3) Eschenmoser, A.; Loewenthal, E. Chemistry of Potentially Prebiological Natural-Products. *Chem. Soc. Rev.* **1992**, *21*, 1−16.
(4) Kamiya, H.; Kasai, H. Formation of 2-Hydroxydeoxyadenosine Triphosphate, an Oxidatively Damaged Nucleotide, and Its Incorporation by DNA-Polymerases-Steady-State Kinetics of the Incorporation. *J. Biol. Chem.* **1995**, *270*, 19446−19450.
(5) MurataKamiya, N.; Kamiya, H.; Muraoka, M.; Kaji, H.; Kasai, H. Comparison of Oxidation Products from DNA Components by Gamma-Irradiation and Fenton-Type Reactions. *J. Radiat. Res.* **1997**, *38*, 121−131.
(6) Kamiya, H.; Kasai, H. Effects of Sequence Contexts on Misincorporation of Nucleotides Opposite 2-Hydroxyadenine. *FEBS Lett.* **1996**, *391*, 113−116.
(7) Kamiya, H.; Kasai, H. Mutations Induced by 2-Hydroxyadenine on a Shuttle Vector During Leading and Lagging Strand Syntheses in Mammalian Cells. *Biochemistry* **1997**, *36*, 11125−11130.
(8) Chen, X. Y.; Kierzek, R.; Turner, D. H. Stability and Structure of Rna Duplexes Containing Isoguanosine and Isocytidine. *J. Am. Chem. Soc.* **2001**, *123*, 1267−1274.
(9) Strazewski, P.; Tamm, C. Replication Experiments with Nucleotide Base Analogs. *Angew. Chem., Int. Ed. Engl.* **1990**, *29*, 36−57.
(10) Switzer, C.; Moroney, S. E.; Benner, S. A. Enzymatic Incorporation of a New Base Pair into DNA and Rna. *J. Am. Chem. Soc.* **1989**, *111*, 8322−8323.
(11) Hitchcock, D. S.; Fedorov, A. A.; Fedorov, E. V.; Dangott, L. J.; Almo, S. C.; Raushel, F. M. Rescue of the Orphan Enzyme Isoguanine Deaminase. *Biochemistry* **2011**, *50*, 5555−5557.
(12) Yao, L. S.; Cukier, R. I.; Yan, H. G. Catalytic Mechanism of Guanine Deaminase: An Oniom and Molecular Dynamics Study. *J. Phys. Chem. B* **2007**, *111*, 4200−4210.
(13) Sponer, J. E.; Miguel, P. J. S.; Rodriguez-Santiago, L.; Erxleben, A.; Krumm, M.; Sodupe, M.; Sponer, J.; Lippert, B. Metal-Mediated Deamination of Cytosine: Experiment and DFT Calculations. *Angew. Chem., Int. Ed.* **2004**, *43*, 5396−5399.
(14) Matsubara, T.; Dupuis, M.; Aida, M. Ab Initio Oniom-Molecular Dynamics (MD) Study on the Deamination Reaction by Cytidine Deaminase. *J. Phys. Chem. B* **2007**, *111*, 9965−9974.
(15) Almatarneh, M. H.; Flinn, C. G.; Poirier, R. A.; Sokalski, W. A. Computational Study of the Deamination Reaction of Cytosine with H_2O and OH^-. *J. Phys. Chem. A* **2006**, *110*, 8227−8234.
(16) Almatarneh, M. H.; Flinn, C. G.; Poirier, R. A. Mechanisms for the Deamination Reaction of Cytosine with H_2O/OH^- and $2H_2O/OH^-$: A Computational Study. *J. Chem. Inf. Mod.* **2008**, *48*, 831−843.
(17) Uddin, K. M.; Almatarneh, M. H.; Shaw, D. M.; Poirier, R. A. Mechanistic Study of the Deamination Reaction of Guanine: A Computational Study. *J. Phys. Chem. A* **2011**, *115*, 2065−2076.
(18) Uddin, K. M.; Poirier, R. A. Computational Study of the Deamination of 8-Oxoguanine. *J. Phys. Chem. B* **2011**, *115*, 9151−9159.
(19) Alrawashdeh, A. I.; Almatarneh, M. H.; Poirier, R. A. Computational Study on the Deamination Reaction of Adenine with OH^-/nH_2O (n = 0, 1, 2, 3) and $3H_2O$. *Can. J. Chem.* **2013**, *91*, 1−9.
(20) Gonzalez, C.; Schlegel, H. B. Reaction-Path Following in Mass-Weighted Internal Coordinates. *J. Phys. Chem.* **1990**, *94*, 5523−5527.
(21) Cances, E.; Mennucci, B.; Tomasi, J. A New Integral Equation Formalism for the Polarizable Continuum Model: Theoretical Background and Applications to Isotropic and Anisotropic Dielectrics. *J. Chem. Phys.* **1997**, *107*, 3032−3041.
(22) Frisch, M. J. ; Trucks, G. W.; Schlegel, H. B.; Scuseria, G. E.; Robb, M. A.; Cheeseman, J. R.; Scalmani, G.; Barone, V.; Mennucci, B.; Petersson, G. A.; et al. *Gaussian03*, Revision A.02; Gaussian, Inc.: Wallingford, CT, 2009.
(23) Chen, Z. Q.; Zhang, C. H.; Kim, C. K.; Xue, Y. Quantum Mechanics Study and Monte Carlo Simulation on the Hydrolytic Deamination of 5-Methylcytosine Glycol. *Phys. Chem. Chem. Phys.* **2011**, *13*, 6471−6483.